Evidence of Self-Organised Criticality in Time Series by the Horizontal Visibility Graph Approach

Bardia Kaki (bardia.kaki@znu.ac.ir)
University of Zanjan
Nastaran Farhang
Isfahan University of Technology
Hossein Safari
University of Zanjan

Article

Keywords: Complex Networks, Horizontal Visibility Graph, Self-Organised Criticality, Time Series Analysis

Posted Date: March 15th, 2022

DOI: https://doi.org/10.21203/rs.3.rs-1434364/v1

Evidence of Self-Organised Criticality in Time Series by the Horizontal Visibility Graph Approach

Bardia Kaki[1,*], **Nastaran Farhang**[2], **and Hossein Safari**[1]

[1]Department of Physics, Faculty of Science, University of Zanjan P.O. Box 45195-313, Zanjan, Iran
[2]Department of Physics, Isfahan University of Technology P.O. Box 84154-83111, Isfahan Iran
[*]bardia.kaki@znu.ac.ir

ABSTRACT

Determination of self-organised criticality (SOC) is crucial in evaluating the dynamical behavior of a time series. Here, we apply the complex network approach to assess the SOC characteristics in synthesis and real-world data sets. To this purpose, we employ the horizontal visibility graph (HVG) method and construct the relevant networks for the observational and numerical avalanching events (e.g., earthquakes and sand-pile models), financial markets, and the solar nano-flare emission model, which showed to have long-temporal correlations via re-scaled range analysis. We compute the degree distribution, maximum eigenvalue, and average clustering coefficient of each HVG and compare them with the values obtained for random and chaotic processes. The result manifests a perceptible deviation between these parameters in random and SOC time series. We conclude that the mentioned HVG's features can distinguish between SOC and random systems.

Keywords: Complex Networks, Horizontal Visibility Graph, Self-Organised Criticality, Time Series Analysis.

Introduction

One of the most important parts of studying natural phenomena is classifying them into groups with the same characteristics. This could provide important information about forecasting capabilities and appropriate computational techniques required for further studies. Even though it seems straightforward at first sight, it is not, and it requires scientists to follow certain processes and strategies[1]. The problem becomes more intricate when there isn't a comprehensive description of the subject system or the phenomenon encompasses a wide range of fields. Complex systems seem to confront with both, because on the one hand there is no all-inclusive interpretation of these systems[2–4], and on the other hand they include everything from brain structure to insect colonies, price fluctuations in financial markets, condensate matter, Internet, Plasma and Solar physics, and even all human societies[3,5–10]. Given the breadth and intricacy mentioned, classifying complex systems is an outstanding issue that has attracted vast research interests[11–14].

One of the most familiar aspects of the complexity science is the nonlinear response of a system to small variations in its initial condition, usually referred to as chaotic behavior[15–17]. This behavior has been repeatedly reported in the literature across various fields including astronomy, biology, chemistry, economy, engineering, geology, *etc*[18,19]. Considering the high sensitivity to initial conditions, identification of chaotic behavior in real-world data is more challenging than in artificial data sets[20]. Another aspect is the theory of SOC, in which a gradual energy supply leads the system to a critical state. Then, the system relaxes through a sequence (avalanche) of nonlinear energy-dissipative events that manifests a power-law-like behavior[5,21–25]. Here, "energy" corresponds to any interaction that could impose a phase transition from an original meta-stable state to another[26], in contrast to the chaotic systems for which no stable state can be considered[27].

Conventionally, a system with slow driving rate and instant relaxations is most likely a SOC system if it could produce a wide range of avalanches with inverse dependence of frequencies on the event sizes. However, some variations from this interpretation have been discussed in the literature[28,29]. The chaotic and SOC systems along with significant differences exhibit some character resemblances and might even behave similarly[30].

To this date, several algorithms have been developed to characterize complex systems[31,32]. One of the most popular techniques is the measure of the Lyapunov's exponent[33,34], which determines how fast a very small distance between two originally close trajectories grows (or decreases) over time[35]. Another technique is to perform a cyclical analysis on time series (TS) and investigate whether the frequency spectrum exhibits a periodic pattern[36–38]. Furthermore, fractal dimension[39,40], Kolmogorov-Sinai entropy[41], and the network approach[42,43] have been widely used in identification and analysis of complex systems. The complex network theory could provide more convenient and manageable tools to conduct TS analysis[44–47].

In the present study, we first validate the complexity of several observational and synthesis TS applying the re-scale range

analysis (R/S). Then, we construct the HVGs of the TS and calculate some of the graphs' properties such as the degree distribution, maximum eigenvalue, and average clustering coefficient. Finally, we assess whether it is possible to distinguish between different categories of complex systems using these features. The reminder of this paper is organized as follows: In Section 1 we explain how the network theory could practically provide an indicator for random TS and discuss the possibility of determining random processes from other types (i.e., chaotic and SOC processes). In Section 2 we introduce several data sets and investigate the utility of the network approach in their identification. Finally, we present conclusions in Section 3.

1 The Classifier Indicator

Applying the complex network approach, Lacasa et al.[48] introduced the visibility graph (VG) method which converts a given TS into a graph. According to this algorithm, the sample data points are regarded as nodes (vertices), and an edge (link) is considered between nodes i and j if the following condition is met:

$$y_c < y_i + (y_j - y_i)\frac{t_c - t_i}{t_j - t_i}, \tag{1}$$

where (t_c, y_c) is a data value placed in between i and j. Further to this algorithm, Luque et al.[49] presented the HVG which to a great extent is analogous to the VG method except for the visibility condition:

$$y_i, y_j > y_c \quad (\text{for all c such that } i < c < j). \tag{2}$$

A major advantage of the HVG method is that it provides the analytical capability to calculate the degree distribution of random series. Therefore, the degree distribution of any random process regardless of the generator type follows a specific distribution:

$$P(k) = \frac{1}{3}\left(\frac{2}{3}\right)^{k-2}, \tag{3}$$

where P and k denote the probability distribution function (PDF) and the degree of nodes, respectively. The probability distribution of Equation (3) could be regarded as an indicator for random series. In other words, if the degree distribution of a given sample follows Equation (3) the underlying mechanism is most likely specified as a random process.

The question is how the degree distribution of other processes behave in comparison with random TS. Luque et al.[49] tried to address this question by performing a study on chaotic systems. They found that the degree distribution of chaotic processes deviate from the random indicator as they have higher probabilities at high degrees. Here, we go one step further and investigate the degree distribution of SOC systems and examine their behavior against the random indicator. Moreover, we calculate the maximum eigenvalues and average clustering coefficients of several SOC systems and evaluate their utility in distinguishing between SOC and random systems. The details of the analysis and the achieved results are discussed in the next section.

2 HVGs of SOC Systems

The main idea is to investigate the SOC characteristics of data samples using the network approach. For this purpose, we construct the HVGs of various SOC systems and compare some of their networks' properties (e.g., degree distribution) with random processes. But, we first need to validate the complexity of each subject TS. Diagnosing the complexity of a system could be accomplished using a variety of methods mainly classified in three categories: Fractality, which investigates the existence of self-similarity or long-term memory in a system; Nonlinear dynamic methods that operate based on evaluation of the attractor properties in the phase space; And the entropy which assesses the disorder in a system[50]. Here, we apply the R/S analysis which measures the variability of a data sample against time[51,52].

In order to measure the possible deviations between the degree distributions of SOC and random TS, we calculate both the orthogonal regression and the Kolmogorov-Smirnov test (KS-test). Considering the random indicator as the reference, degrees with higher (lower) probabilities than the indicator are assigned with positive (negative) distances. Therefore, the sum of all distances specifies whether the subject system behaves randomly (approximate zero deviation), chaotically (positive deviation), or it represents SOC (negative deviation). Further to the degree distribution, we measure each network's maximum eigenvalue which has been acknowledged as an efficient method to distinct between chaotic and random TS[53,54]. Here, we appraise its capability in determining SOC systems. We also compute the average clustering coefficients[6,7,10,55,56] of the HVGs and compare the outcomes with random processes.

We start our survey with the most celebrated SOC system, namely the sand-pile model[57]. This model employs a grid over which sand grains are initially randomly distributed. At each time step a grain falls into a randomly selected square.

The whole system is conned to a stability criterion that depends on the heights of nearest neighbors. Whenever a square does not contain enough capacity to accommodate the new grain (the height exceeds a pre-xed threshold), the grain ows into neighboring squares or ejects from the corners of the grid to locally relax the system.

We reproduce the sand-pile model using both the original Bak redistribution rules and those introduced by Manna (Figure 2)[58]. The result of the R/S analysis for both sand-pile models are presented in Figure 1. The measured Hurst exponents of two random TS are also shown in the figure. As observed, the empirical Hurst exponents of the sand-pile models deviate from the theoretical slope of 0.5 whereas the calculated values for random TS matches with theoretical line. This confirms the complexity of the sand-pile systems. The degree distribution of both sand-pile models' HVGs together with the theoretical distribution of random systems (Equation 3) are shown in Figure 3. As seen in the figure, most of the degrees (specially the high degrees) have less probabilities than the random indicator. The total deviation between the Bak and Manna sand-pile models and the indicator are -5.9417 and -5.7680, respectively. The orthogonal distances are measured in the logarithmic scale.

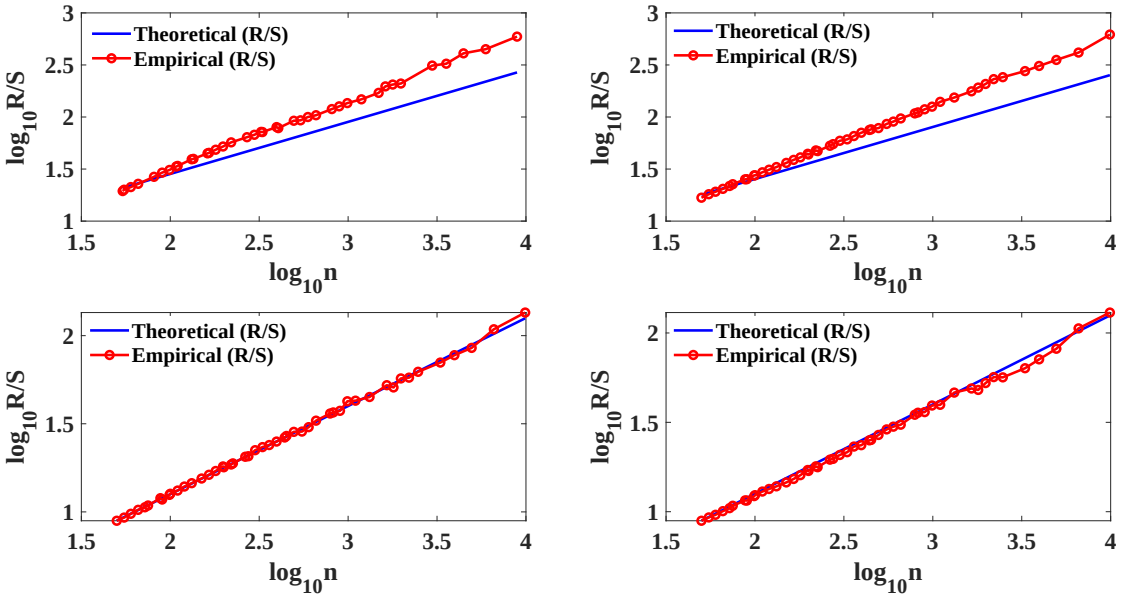

Figure 1. Estimation of the Hurst exponent using the R/S analysis for: Manna sand-pile model (top left panel), Bak sand-pile model (top right panel), uniformly distributed random series (bottom left panel), and a normally distributed random series (bottom right panel).

Figure 4 displays the maximum eigenvalues of both sand-pile models together with the relevant values for some random and chaotic processes. The random TS are constructed using the uniform and normal generators whilst the chaotic TS correspond to a logistic map $x_{t+1} = \mu x_t(1-x_t)$ and the Hénon map $(x_{t+1}, y_{t+1}) = (y_{t+1} - ax_t^2, bx_t)$ in a fully chaotic region with $\mu = 4, a = 1.4$, and $b = 0.3$. As shown in the figure, the maximum eigenvalues slightly increase for the network's size. For a convenient network with a total number of nodes greater than 2500, the maximum eigenvalues of a random and chaotic TS lie approximately in the ranges of $7-7.7$ and $7.8-8.7$, respectively. Whilst, the maximum eigenvalues of Bak and Manna sand-pile models are in the range of $5.5-6.3$. The average clustering coefficients[6,7,10,55,56] of mentioned TS are also presented in Figure 5. Likewise the maximum eigenvalues, the average clustering coefficients of both sand-pile models are distinguishable from the random and chaos processes.

So far, we have obtained that the HVGs of individual categories seem to have distinctive characteristics. This raise the question whether these properties (i.e., degree distribution, maximum eigenvalue, and average clustering coefficient) could practically be used as an indicator to identify SOC systems. To address this question, we examine several other SOC systems in the following.

Inspired by the power-law-like behavior of the solar flare energies, Tajfirouze and Safari[59] presented a SOC model to investigate the complex evolution of nano-flare emissions in the quiet Sun and active regions. The nano-flare emission model is controlled by three free parameters, namely the power index α, damping time τ_d, and the occurrence probability of flaring

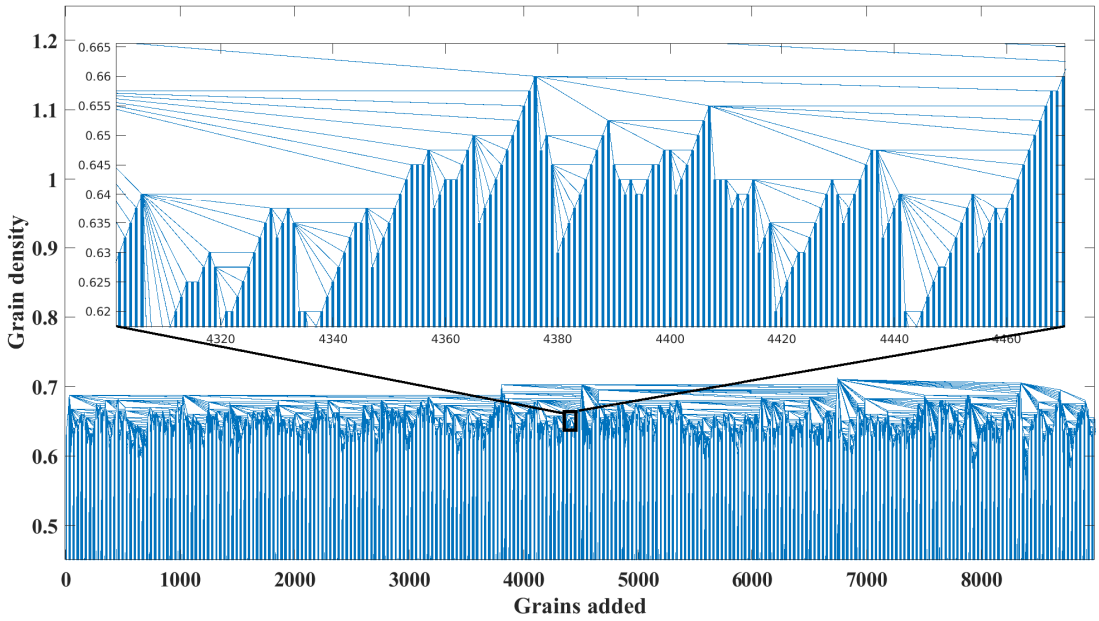

Figure 2. The HVG for the Manna sand-pile model with 9,000 grains.

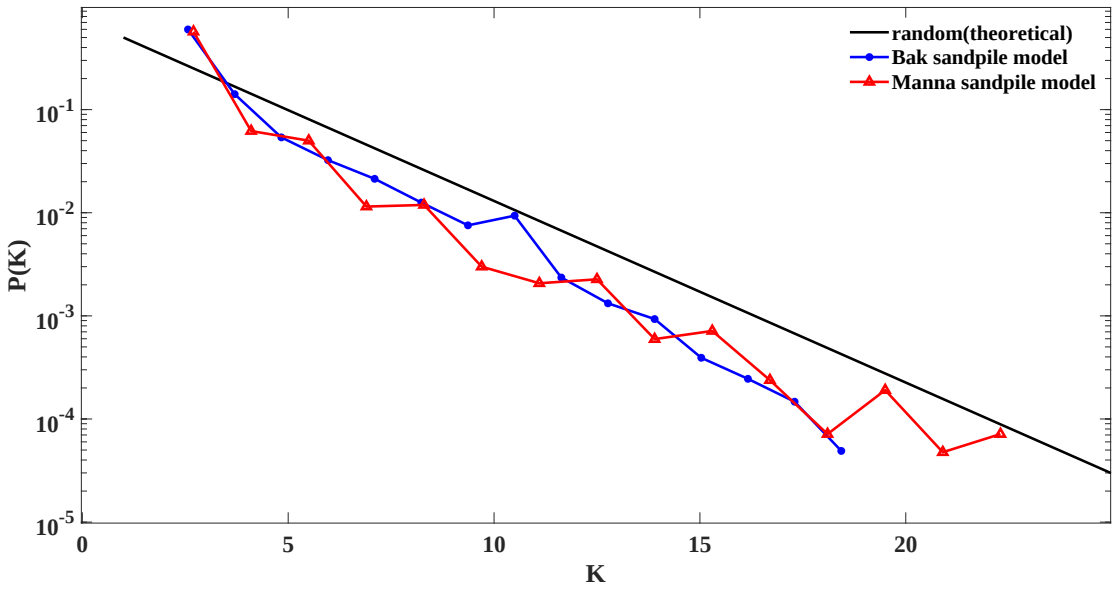

Figure 3. Semi-logarithmic presentation of PDFs of the degree of nodes for: any random process (solid black line) which follows Equation (3), the Bak (blue line), and Manna (red line) sand-pile models.

events p_f[60–62]. The parameter α is the power index in the frequency-size distribution of flare energies (E):

$$\frac{dN}{dE} \propto E^{-\alpha}. \tag{4}$$

The reported values for this parameter in solar and stellar flares lies between 1.5 and 2.9[23,24,60,62–71]. τ_d corresponds to the flare damping time and various choice of τ_d could affect the overall shape of the flares' frequency-size distribution. For example, the adoption of large values for this parameter leads to a Gaussian frequency-size distribution rather than a power

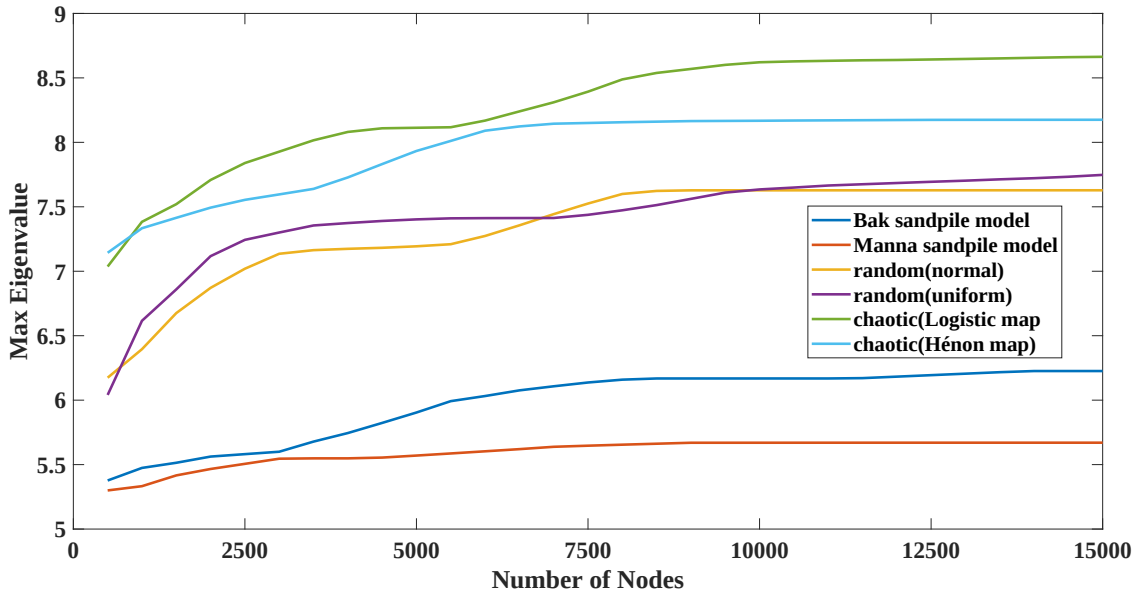

Figure 4. The maximum eigenvalues against the number of nodes for constructed network for different TS.

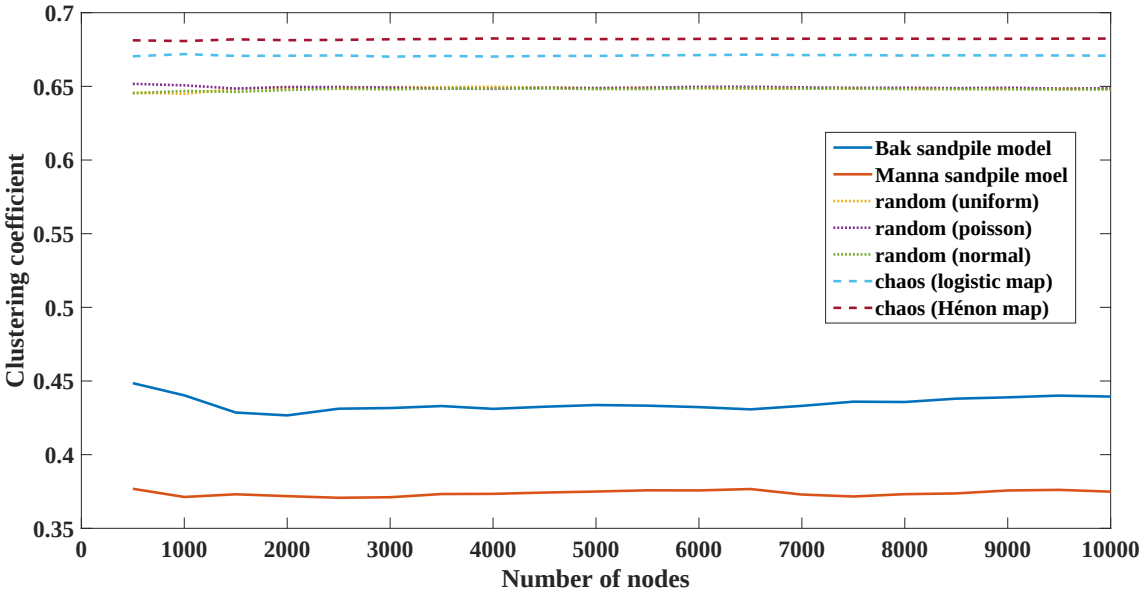

Figure 5. The average clustering coefficient for the Bak (solid blue line) and Manna (solid red line) models, several random TS (dotted colored lines) and two chaotic TS (dashed colored line).

law. The parameter p_f corresponds to the likelihood of a flare taking place and can take all values between 0 and 1. Figure 6 displays the simulated light curves of the nano-flare emission model for different sets of parameters ($\alpha \in [1.4\ 3.2]$, $\tau_d = 10$, and $p_f < 0.2$).

Figures 7 and 8 present the result of the R/S analysis and the degree distributions of the simulated light curves, respectively. The calculated Hurst exponents confirms the complexity of the simulated TS. All degree distributions exhibit a negative orthogonal regression from the random indicator. The deviation between each degree distribution and the indicator together with the maximum eigenvalues, and average clustering coefficients of each simulation are listed in Table 1. The results are compatible with the sand-pile models. The reported values are obtained by taking the average and standard deviations of each

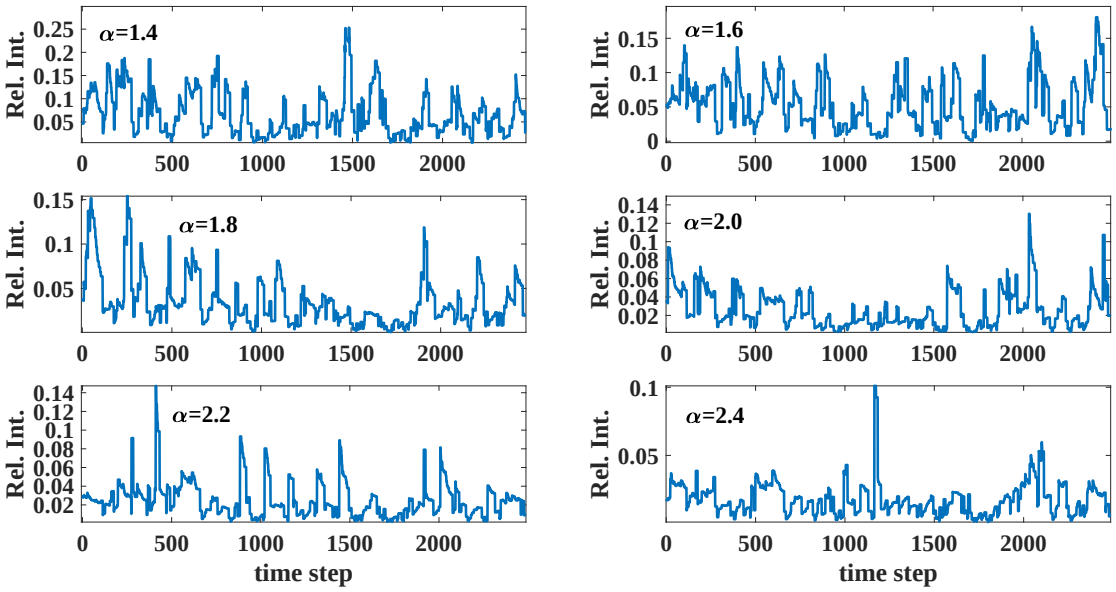

Figure 6. Simulated light curves of the nano-are emission model for $\tau_d = 10$, $p_f = 0.2$, and different α values.

parameter for various sets of runs. Note that the procedure of repeating the calculations is not generally applicable to the real-world data sets except for conveniently large data samples.

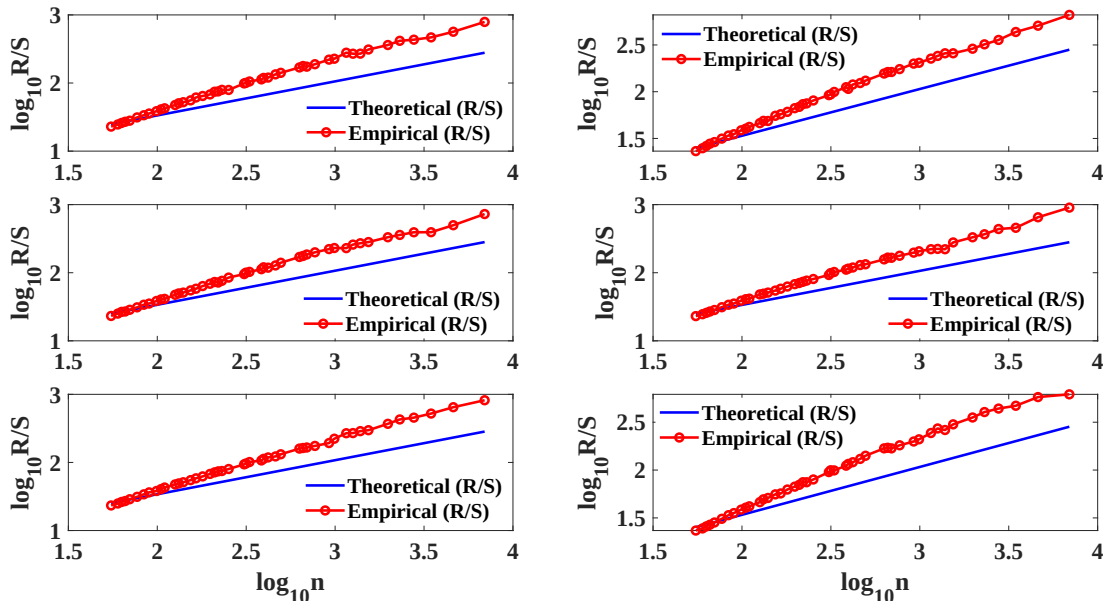

Figure 7. Estimation of the Hurst exponent using the R/S analysis for the simulated light curves of the nano-flare emission model with $\alpha = 1.4, 1.6, 1.8, 2, 2.2, 2.4$.

As another example, we construct the HVG of the complex system of earthquakes which has been generally accepted as a SOC system[26,72]. In order to do so, we use the United States Geological Survey (USGS) data archive which is online available at https://earthquake.usgs.gov/earthquakes/search. The archive includes the information of 15,550 earthquakes occurred all around the world between 30 January, 2020 and 30 January, 2022, with magnitudes of $m > 4.5$. The left panel of Figure 9 presents the result of the R/S analysis for this TS and indicates the complexity of the system of earthquakes. Figure 10 shows the degree distribution of the earthquakes' HVG. The distribution exhibits a

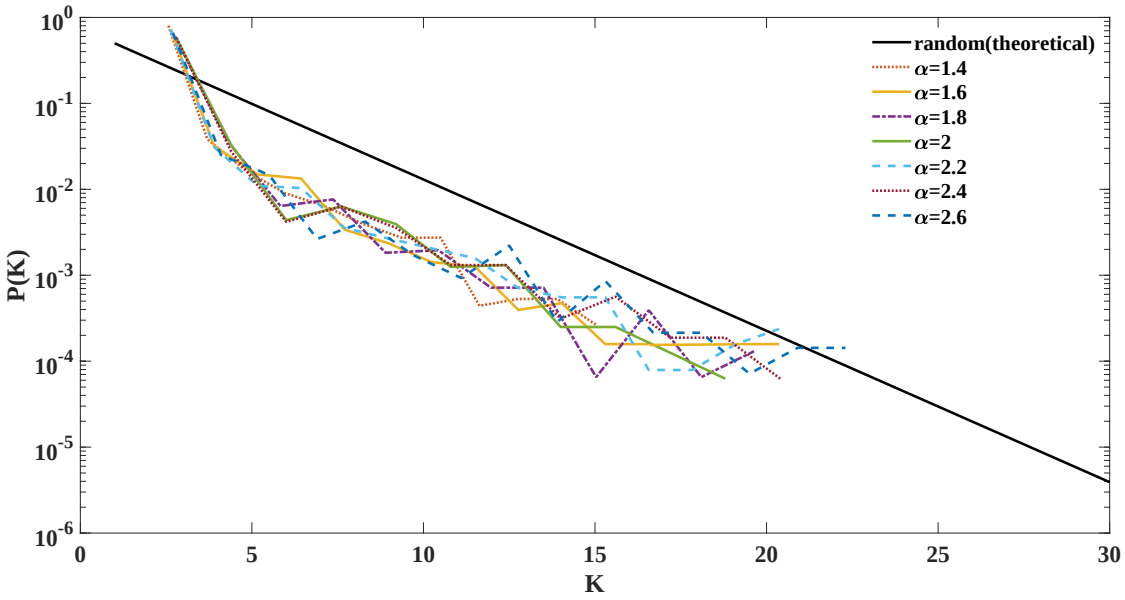

Figure 8. Semi-logarithmic presentation of PDFs of the degree of nodes for: any random process (solid black line) which follows Equation (3), and various runs of simulation of the nano-flare emission model with $\alpha \in [1.4\ 3.2]$, $\tau_d = 10$, and $p_f = 0.2$.

Table 1. General properties of the constructed HVGs (with 14000 nodes) for the nano-flare emission model. The model parameters are $\alpha \in [1.4\ 3.2]$, $\tau_d = 10$, and $p_f < 0.2$.

α	Orthogonal distances	Maximum eigenvalue	Clustering Coefficient
1.4	-11.3022	5.47±0.16	0.27±0.01
1.6	-10.3042	5.64±0.20	0.27±0.01
1.8	-7.9483	6.51±0.21	0.28±0.01
2	-7.1418	6.03±0.24	0.28±0.01
2.2	-6.9388	6.05±0.16	0.27±0.01
2.4	-6.2146	6.38±0.26	0.27± 0.01
2.6	-5.0290	6.32±0.39	0.23 ± 0.01

downward deviation (negative distance of -4.3980) from the random indicator. The maximum eigenvalue and the average clustering coefficient are also computed as 6.86 ± 0.1002 and 0.42 ± 0.0013, respectively.

Further to the USGS data, we also construct the HVG of 5,250 earthquakes occurred in the North America between 03 July, 1841 to 25 February, 2022. The right panel of Figure 9 shows the measured Hurst exponent for this data sample which expectedly presents the complexity of the earthquakes TS. The orthogonal distance (Figure 11), maximum eigenvalue and average clustering coefficient are obtained -2.55, 7.09, and 0.55, respectively. Based on the achieved results, the investigated properties of the SOC system of earthquakes clearly diverge from random systems.

We continue our survey by performing the same analysis on various financial data sets as other examples of SOC systems[22,73]. The dynamics of price movements or other indices of the financial markets are determined by the behavior of individuals who act based on their information[73]. Here, we investigate the historical price of several assets (such as gold, different company stocks, and commodities), as well as several economic indices (such as the Nasdaq 100, S&P 500, and U.S. dollar index). These information are registered in the Stooq Database and are online available at https://stooq.com/. We construct the HVGs for the maximum amounts of available data and the daily frequencies. Figure 12 exhibits the result of the R/S analysis for the financial TS. The Hurst exponents of these series manifest the complex nature of these systems. Figure 13 displays the relevant degree distributions. The obtained orthogonal distances, maximum eigenvalues, and the average clustering coefficients of each HVG are presented in Table 2. Similar to previous SOC systems, the estimated parameters are less than the relevant values of random systems. However, the departures between the financial HVG's clustering coefficients and the random systems are less significant comparing to the sand-pile and nano-flare emission models.

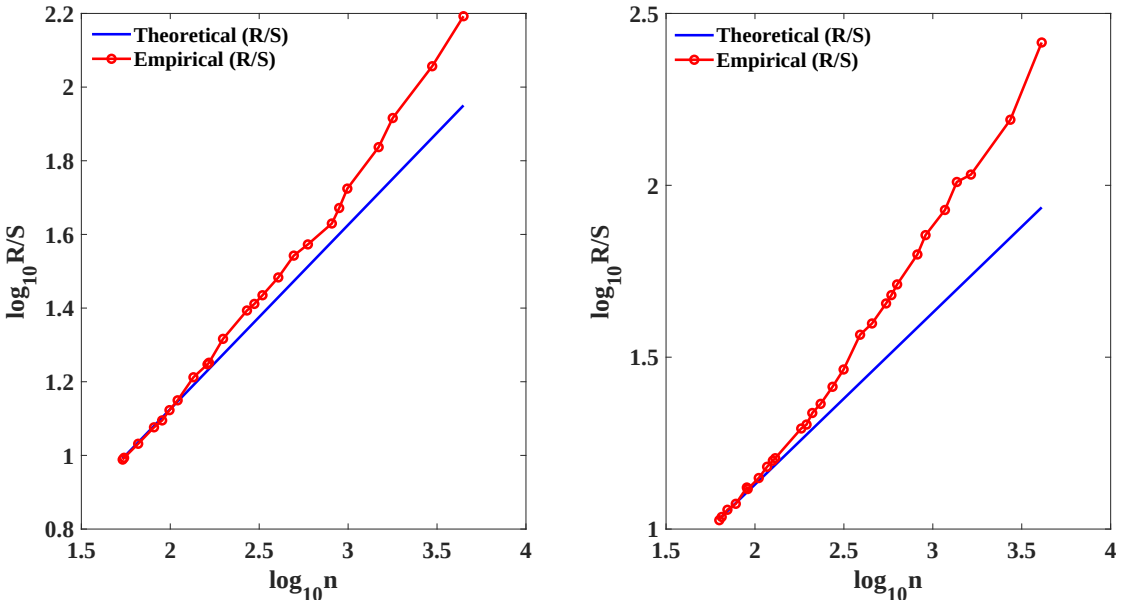

Figure 9. Estimation of the Hurst exponent using the R/S analysis for the recorded earthquakes all over the world with a magnitude of $m > 4.5$ and the recorded earthquakes in the North America with a magnitude of $m > 4.5$.

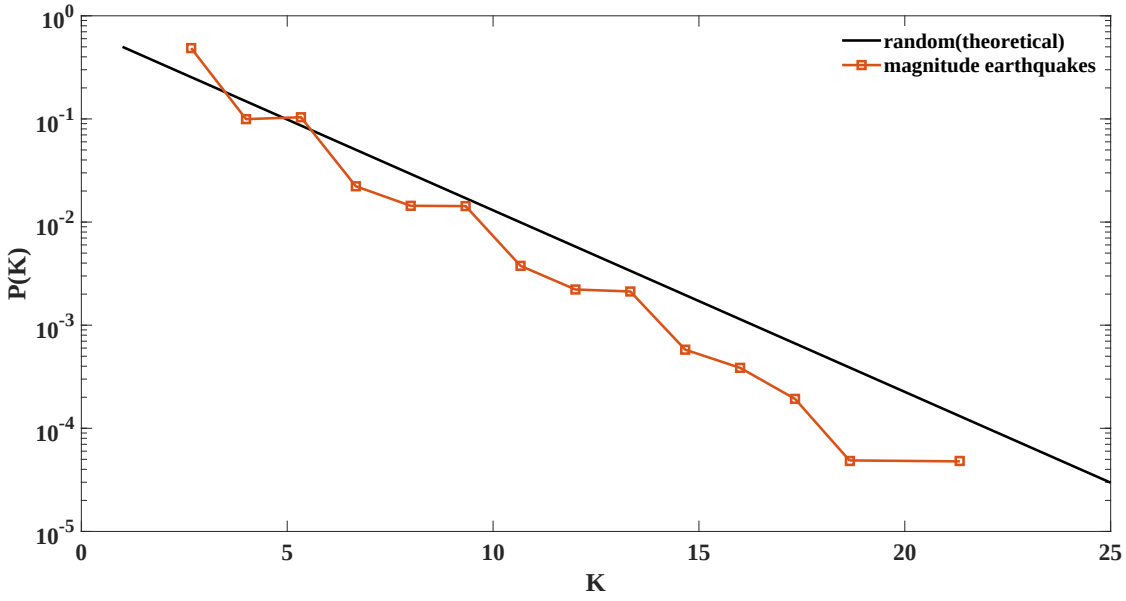

Figure 10. Semi-logarithmic presentation of PDFs of the degree of nodes for: any random process (solid black line) which follows Equation (3), and recorded earthquakes all over the world with a magnitude of $m > 4.5$ between 30 January, 2020 and 30 January, 2022 (red line).

Further to calculation of orthogonal distances, we apply the KS-test to compare the degree distribution of constructed HVGs with the random indicator (null hypothesis). The KS-test returns the test statistic (t-stat, the ratio of the departure between a specific model and the indicator to its standard deviation) and the p-value (p)[74–76]. For $p > 0.1$ (threshold), reject the null hypothesis that shows a degree distribution for a specific model may not obey the random indicator. Table 3 presents the obtained t-test sand p-values for various random and SOC TS. As expected, the t-test values for both degree distributions of the normal and power-law random models satisfy the random indicator that are not rejected by p-values ($p > 0.1$). We

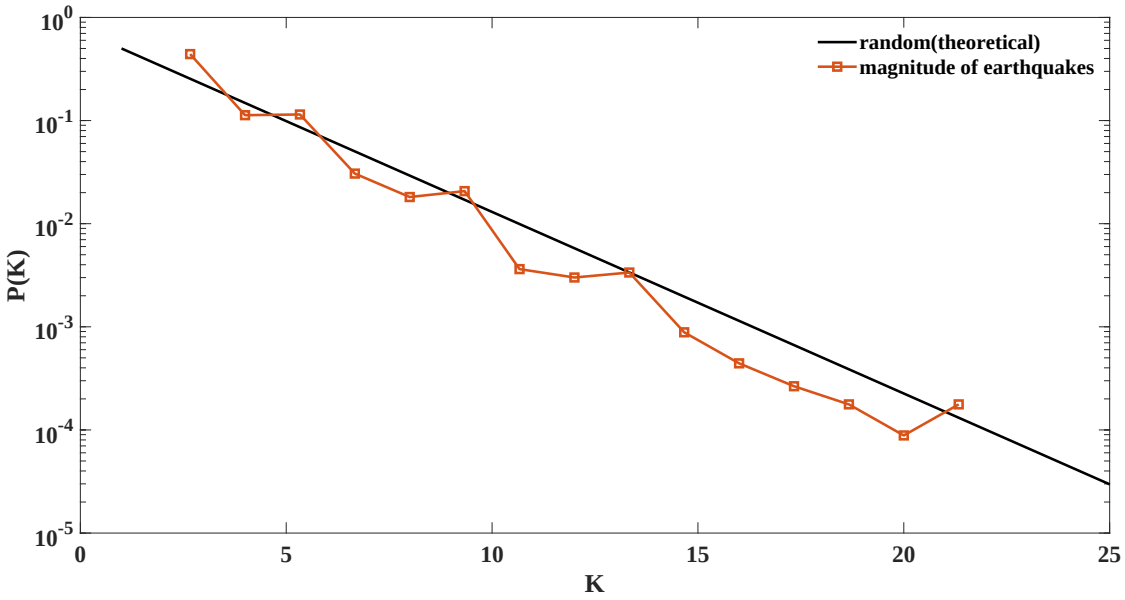

Figure 11. Semi-logarithmic presentation of PDFs of the degree of nodes for: any random process (solid black line) which follows Equation (3), and recorded earthquakes in the North America with a magnitude of $m > 4.5$ between 03 July, 1841 to 25 February, 2022.

Table 2. General properties of the financial TS HVGs.

Financial instrument	No. of Nodes	Orthogonal Distances	Maximum Eigenvalue	Average Clustering Coefficient
Euro / U.S. Dollar	13070	-4.4967	5.7887	0.5875
Gold (ozt) / U.S. Dollar	14122	-4.9621	6.3913	0.5418
Microsoft Corp	9047	-6.4082	6.1790	0.5082
Nasdaq 100 Indicies	9162	-4.3530	6.3112	0.5922
S&P 500	19643	-5.3937	6.5304	0.5979
U.S. Dollar Index	13035	-5.0453	5.9480	0.5860

observed that the degree distribution of the SOC TS are deviated from the random indicator that are also rejected with the null hypothesis via the small p-values ($p < 0.1$).

3 Discussion

In this article, we investigated the utility of the HVG in identifying the SOC characteristics of artificial and real-world data sets. We first constructed the HVGs of the Bak and Manna sand-pile models, the nano-flare emission model, earthquakes, and financial markets. Then, we validated the complexity of each system by calculating their Hurst exponents. Based on the applied R/S analysis, we confirmed that all studied TS differed from any random uncorrelated TS. We also computed the degree distribution, maximum eigenvalue, and average clustering coefficient of each HVG and compared them with the relevant values for random processes.

Considering the Equation (3) as an indicator for any random process, we obtained the degree distributions of several SOC systems' HVGs and evaluated their deviations from the random indicator. In all the studied TS, we found a negative orthogonal distance between the degree distribution of the subject system and the indicator. In other words, we found that higher degrees are less probable in SOC systems rather than random processes. Therefore, an increase in the probability of high degrees indicates a transition from SOC to randomness or even chaos.

We found that the HVG's maximum eigenvalues of any random process with at least 2500 data samples lie in the range of $7 - 7.8$. However, the maximum eigenvalues of all the studied SOC systems are between $5.5 - 6.5$. Similar departures are found between the average clustering coefficients of SOC and random processes. We conclude that the HVG is a useful tool

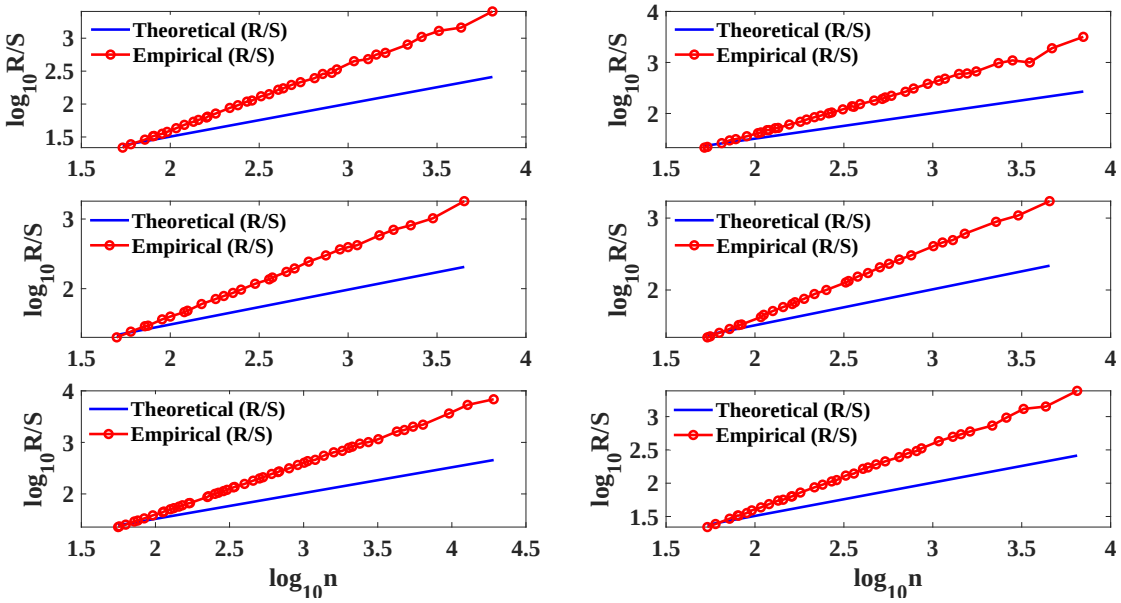

Figure 12. Estimation of the Hurst exponent using the R/S analysis for the exchange rate for euros to dollars (Euro / U.S. Dollar 1:1), gold price per ozt (Gold (ozt) / U.S. Dollar 1:1), Microsoft corp stock price, NASDAQ 100 index , *S&P* 500 index, U.S. dollar index.

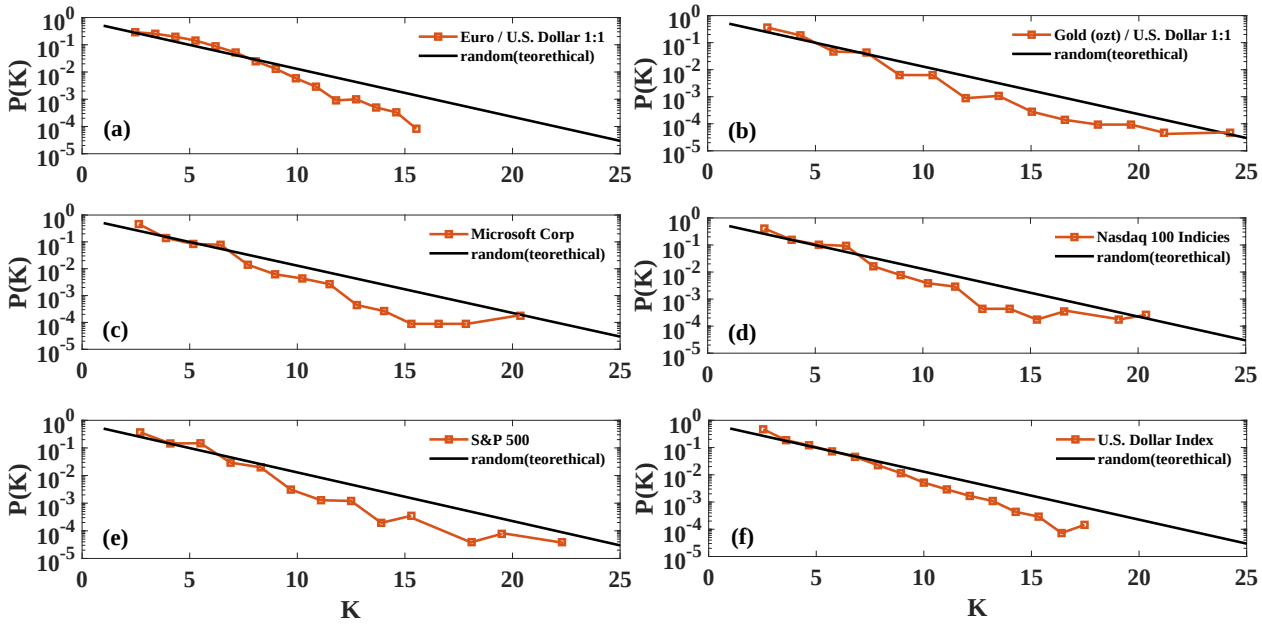

Figure 13. Semi-logarithmic presentation of PDFs of the degree of nodes for: any random process (solid black line) which follows Equation (3), the exchange rate for euros to dollars (Euro / U.S. Dollar 1:1) from 04 January 1971 till 23 July 2021, gold price per ozt (Gold (ozt) / U.S. Dollar 1:1) from 01 March 1793 till 23 July 2021, Microsoft corp stock price from 13 March 1986 till 23 July 2021, NASDAQ 100 index from 1 October 1985 till 23 July 2021, S&P 500 index from 2 January 1952 till 23 July 2021, U.S. dollar index from 4 January 1971 till 23 July 2021.

in identifying SOC systems as its features (degree distribution, maximum eigenvalue, and average clustering coefficient) are distinguishable from random and chaotic TS.

Table 3. The result of the KS-test for all studied TS. The two last columns of the table present the t-tests and p-values for which the null hypothesis (random indicator) is accepted/rejected.

TS	t-test value	p-values
Random power-law	0.0049	0.9998
Random normal	0.0041	0.9984
Bak	0.1358	<0.0001
Manna	0.2452	<0.0001
Chaos logistic map	0.1127	<0.0001
Chaos Hénon map	0.0777	<0.0001
α=1.4	0.4546	<0.0001
α=1.6	0.4513	<0.0001
α=1.8	0.4482	<0.0001
α=2	0.4497	<0.0001
α=2.2	0.4506	<0.0001
α=2.4	0.4480	<0.0001
α=2.6	0.4457	<0.0001
World earthquake	0.1006	<0.0001
USA earthquake	0.0336	$\sim$ 0.0001
Euro / U.S. Dollar	0.0621	<0.0001
Gold (ozt) / U.S. Dollar	0.0407	<0.0001
Microsoft Corp	0.0640	<0.0001
Nasdaq 100 Indicies	0.0617	<0.0001
S & P 500	0.0746	<0.0001
U.S. Dollar Index	0.0786	<0.0001

Acknowledgements

Authors would like to thank the United States Geological Survey archive and the Stooq Database for sharing their information. Nastaran Farhang express her gratitude to the Iran National Science Foundation (INSF) for supporting this research under grant No. 99012824.

Author contributions statement

B.K. conceived of the presented idea. H.S. and N.F. were involved in designing the study and supervised the work. B.K. worked out almost all of the computations. All authors contributed to the analysis of the results and to the writing of the manuscript.

Data Availability Statement

The data for sand-pile and nano-flare emission models that support the findings of this study are available from the authors upon request [bardia.kaki@znu.ac.ir and safari@znu.ac.ir].

The earthquake data that support the findings of this study are available from [https://earthquake.usgs.gov/earthquakes/search].

The financial markets data that support the findings of this study are available from [https://stooq.com/].

References

1. Szostak, R. *Classifying science - phenomena, data, theory, method, practice*, vol. 7 of *Information science and knowledge management* (Springer, 2004).

2. Solé, R. V., Manrubia, S. C., Luque, B., Delgado, J. & Bascompte, J. Phase transitions and complex systems: Simple, nonlinear models capture complex systems at the edge of chaos. *Complexity* **1**, 13–26, DOI: https://doi.org/10.1002/cplx.6130010405 (1996).

3. Newman, M. E. J. Resource Letter CS1: Complex Systems. *Am. J. Phys.* **79**, 800+, DOI: 10.1119/1.3590372 (2011).

4. Siegelmann, H. Complex systems science and brain dynamics. *Front. Comput. Neurosci.* **4**, DOI: 10.3389/fncom.2010.00007 (2010).

5. Pinto, C. M., Mendes Lopes, A. & Machado, J. T. A review of power laws in real life phenomena. *Commun. Nonlinear Sci. Numer. Simul.* **17**, 3558–3578, DOI: https://doi.org/10.1016/j.cnsns.2012.01.013 (2012).

6. Gheibi, A., Safari, H. & Javaherian, M. The solar flare complex network. *The Astrophys. J.* **847**, 115, DOI: 10.3847/1538-4357/aa8951 (2017).

7. Daei, F., Safari, H. & Dadashi, N. Complex network for solar active regions. *The Astrophys. J.* **845**, 36, DOI: 10.3847/1538-4357/aa7ddf (2017).

8. Caldarelli, G. Review of Introduction to the Theory of Complex Systems by Stefan Thurner, Rudolf Hanel and Peter Klimek. *J. Complex Networks* **8**, DOI: 10.1093/comnet/cnz038 (2019).

9. Lotfi, N., Javaherian, M., Kaki, B., Darooneh, A. H. & Safari, H. Ultraviolet solar flare signatures in the framework of complex network. *Chaos* **30**, 043124, DOI: 10.1063/1.5129433 (2020).

10. Mohammadi, Z., Alipour, N., Safari, H. & Zamani, F. Complex network for solar protons and correlations with flares. *J. Geophys. Res. Space Phys.* **126**, e2020JA028868, DOI: https://doi.org/10.1029/2020JA028868 (2021).

11. Crosby, R. W. Toward a classification of complex systems. *Eur. J. Oper. Res.* **30**, 291–293, DOI: https://doi.org/10.1016/0377-2217(87)90073-7 (1987).

12. Meyer, M. H. & Curley, K. F. An applied framework for classifying the complexity of knowledge-based systems. *MIS Q.* **15**, 455–472, DOI: https://doi.org/10.2307/249450 (1991).

13. Korbel, J., Hanel, R. & Thurner, S. Classification of complex systems by their sample-space scaling exponents. *New J. Phys.* **20**, 093007, DOI: 10.1088/1367-2630/aadcbe (2018).

14. Hudcová, B. & Mikolov, T. Classification of complex systems based on transients. In *Classification of Complex Systems Based on Transients*, 367–375, DOI: 10.1162/isal_a_00260 (2020).

15. Lorenz, E. N. Deterministic nonperiodic flow. *J. Atmospheric Sci.* **20**, 130 – 141, DOI: 10.1175/1520-0469(1963)020<0130:DNF>2.0.CO;2 (1963).

16. Cencini, M., Cecconi, F. & Vulpiani, A. *Chaos: From Simple Models to Complex Systems*. Series on advances in statistical mechanics (World Scientific, 2010).

17. Icha, A. Book review: Chaos in nature, by christophe letellier, world scientific series on nonlinear science, series a, vol. 81, series editor leon o. chua, world scientific, 2013; isbn: 978-981-4374-42-2. *Pure Appl. Geophys.* **171**, 1593–1595, DOI: 10.1007/s00024-013-0700-z (2014).

18. Strogatz, S. H. *Nonlinear Dynamics And Chaos: With Applications To Physics, Biology, Chemistry, And Engineering* (Westview Press, Cambridge, 2000).

19. Rutherford, A. *Systems Thinking and Chaos: Simple Scientific Analysis on How Chaos and Unpredictability Shape Our World (and How to Find Order in It)* (Independently Published, 2019).

20. Toker, D., Sommer, F. T. & DEsposito, M. A simple method for detecting chaos in nature. *Commun. Biol.* **3**, 1–13, DOI: https://doi.org/10.1038/s42003-019-0715-9 (2020).

21. Bak, P. *How Nature Works: The Science of Self-Organized Criticality*, vol. 1 (Copernicus, New York, 1996).

22. Bartolozzi, M., Leinweber, D. & Thomas, A. Self-organized criticality and stock market dynamics: an empirical study. *Phys. A: Stat. Mech. its Appl.* **350**, 451–465, DOI: https://doi.org/10.1016/j.physa.2004.11.061 (2005).

23. Farhang, N., Safari, H. & Wheatland, M. S. Principle of minimum energy in magnetic reconnection in a self-organized critical model for solar flares. *The Astrophys. J.* **859**, 41, DOI: 10.3847/1538-4357/aac01b (2018).

24. Farhang, N., Wheatland, M. S. & Safari, H. Energy Balance in Avalanche Models for Solar Flares. *astrophysical journal letters* **883**, L20, DOI: 10.3847/2041-8213/ab40c3 (2019).

25. Tebaldi, C. Self-organized criticality in economic fluctuations: The age of maturity. *Front. Phys.* **8**, 658, DOI: 10.3389/fphy.2020.616408 (2021).

26. Bak, P. & Chen, K. Self-organized criticality. *Sci. Am.* **264**, 46–53 (1991).

27. Gang, H. & Zhilin, Q. Controlling spatiotemporal chaos in coupled map lattice systems. *prl* **72**, 68–71, DOI: 10.1103/PhysRevLett.72.68 (1994).

28. Jeldtoft, J. H. *Self-Organized Criticality: Emergent Complex Behavior in Physical and Biological Systems*. Cambridge Lecture Notes in Physics (Cambridge University Press, 1998).

29. Sornette, D. *Critical Phenomena in Natural Sciences: Chaos, Fractals, Selforganization and Disorder: Concepts and Tools*. Springer Series in Synergetics (Springer Berlin Heidelberg, 2006).

30. Turcotte, D. L. Self-organized criticality: Does it have anything to do with criticality and is it useful? *Nonlinear Processes in Geophysics* **8**, 193–196 (2001).

31. Aguirre, L. A. & Letellier, C. Modeling nonlinear dynamics and chaos: A review. *Math. Probl. Eng.* **2009**, 1–35, DOI: 10.1155/2009/238960 (2009).

32. Uthamacumaran, A. A review of dynamical systems approaches for the detection of chaotic attractors in cancer networks. *Patterns* **2**, 100226, DOI: https://doi.org/10.1016/j.patter.2021.100226 (2021).

33. Wolf, A., Swift, J. B., Swinney, H. L. & Vastano, J. A. Determining lyapunov exponents from a time series. *Phys. D: Nonlinear Phenom.* **16**, 285–317, DOI: https://doi.org/10.1016/0167-2789(85)90011-9 (1985).

34. Shi, W. Lyapunov exponent analysis to chaotic phenomena of marine power system. In Zhang, H.-Y. (ed.) *Fault Detection, Supervision and Safety of Technical Processes 2006*, 1497–1502, DOI: https://doi.org/10.1016/B978-008044485-7/50251-7 (Elsevier Science Ltd, Oxford, 2007).

35. Eckhardt, B. & Yao, D. Local lyapunov exponents in chaotic systems. *Phys. D: Nonlinear Phenom.* **65**, 100–108, DOI: https://doi.org/10.1016/0167-2789(93)90007-N (1993).

36. Dumont, R. S. & Brumer, P. Characteristics of power spectra for regular and chaotic systems. *jcp* **88**, 1481–1496, DOI: 10.1063/1.454126 (1988).

37. Valsakumar, M. C., Satyanarayana, S. V. M. & Sridhar, V. Signature of chaos in power spectrum. *Pramana* **48**, 69–85, DOI: 10.1007/BF02845623 (1997).

38. Jiang, W., Kong, X. & Zhang, Q. Chaotic signal pattern recognition using orthogonal wavelet packet method. *SAE Transactions* **111**, 256–261 (2002).

39. Theiler, J. Estimating fractal dimension. *J. Opt. Soc. Am. A* **7**, 1055–1073, DOI: 10.1364/JOSAA.7.001055 (1990).

40. Freistetter, F. Fractal Dimensions as Chaos Indicators. *Celest. Mech. Dyn. Astron.* **78**, 211–225 (2000).

41. Frigg, R. In what sense is the kolmogorov-sinai entropy a measure for chaotic behaviour?–bridging the gap between dynamical systems theory and communication theory. *Br. J. for Philos. Sci.* **55**, DOI: 10.1093/bjps/55.3.411 (2004).

42. Zhang, J. & Small, M. Complex network from pseudoperiodic time series: Topology versus dynamics. *Phys. review letters* **96**, 238701, DOI: 10.1103/PhysRevLett.96.238701 (2006).

43. Li, C., Lu, J. & Chen, G. Network analysis of chaotic dynamics in fixed-precision digital domain. In *2019 IEEE International Symposium on Circuits and Systems (ISCAS)*, 1–5, DOI: 10.1109/ISCAS.2019.8702232 (2019).

44. Yang, Y. & Yang, H. Complex network-based time series analysis. *Phys. A: Stat. Mech. its Appl.* **387**, 1381–1386, DOI: https://doi.org/10.1016/j.physa.2007.10.055 (2008).

45. Barabási, A.-L. The network takeover. *Nat. Phys.* **8**, 14–16, DOI: 10.1038/nphys2188 (2012).

46. Manshour, P. Complex network approach to fractional time series. *Chaos* **25**, 103105, DOI: 10.1063/1.4930839 (2015).

47. Mata, A. S. Complex Networks: a Mini-review. *Braz. J. Phys.* **50**, 658–672, DOI: 10.1007/s13538-020-00772-9 (2020).

48. Lacasa, L., Luque, B., Ballesteros, F., Luque, J. & Nuño, J. C. From time series to complex networks: The visibility graph. *Proc. Natl. Acad. Sci.* **105**, 4972–4975, DOI: 10.1073/pnas.0709247105 (2008).

49. Luque, B., Lacasa, L., Ballesteros, F. & Luque, J. Horizontal visibility graphs: Exact results for random time series. *pre* **80**, 046103, DOI: 10.1103/PhysRevE.80.046103 (2009).

50. Jebb, A. T., Tay, L., Wang, W. & Huang, Q. Time series analysis for psychological research: examining and forecasting change. *Front. Psychol.* **6**, DOI: 10.3389/fpsyg.2015.00727 (2015).

51. Hurst, H. E. Long-term storage capacity of reservoirs. *Transactions Am. society civil engineers* **116**, 770–799, DOI: https://doi.org/10.1061/TACEAT.0006518 (1951).

52. Weron, R. Estimating long-range dependence: finite sample properties and confidence intervals. *Phys. A: Stat. Mech. its Appl.* **312**, 285–299, DOI: https://doi.org/10.1016/S0378-4371(02)00961-5 (2002).

53. Fioriti, V., Tofani, A. & Pietro, A. D. Discriminating chaotic time series with visibility graph eigenvalues. *Complex Syst.* **21**, DOI: 10.25088/complexsystems.21.3.193 (2012).

54. Flanagan, R., Lacasa, L. & Nicosia, V. On the spectral properties of feigenbaum graphs. *J. Phys. A: Math. Theor.* **53**, 025702, DOI: 10.1088/1751-8121/ab587f (2019).

55. Barabási, A.-L. & Bonabeau, E. Scale-free networks. *Sci. Am.* **288**, 60–69, DOI: 10.2307/26060284 (2003).

56. Najafi, A., Darooneh, A. H., Gheibi, A. & Farhang, N. Solar flare modified complex network. *The Astrophys. J.* **894**, 66, DOI: 10.3847/1538-4357/ab8301 (2020).

57. Bak, P., Tang, C. & Wiesenfeld, K. Self-organized criticality: An explanation of the 1/f noise. *Phys. Rev. Lett.* **59**, 381–384, DOI: 10.1103/PhysRevLett.59.381 (1987).

58. Manna, S. S. Two-state model of self-organized criticality. *J. Phys. A Math. Gen.* **24**, L363–L369, DOI: 10.1088/0305-4470/24/7/009 (1991).

59. Tajfirouze, E. & Safari, H. Can a nanoflare model of extreme-ultraviolet irradiances describe the heating of the solar corona? *The Astrophys. J.* **744**, 113, DOI: 10.1088/0004-637x/744/2/113 (2011).

60. Pauluhn, A. & Solanki, S. K. A nanoflare model of quiet Sun EUV emission. *aap* **462**, 311–322, DOI: 10.1051/0004-6361:20065152 (2007).

61. Safari, H., Innes, D. E., Solanki, S. K. & Pauluhn, A. Nanoflare model of emission line radiance distributions in active region coronae. In Kneer, F., Puschmann, K. G. & Wittmann, A. D. (eds.) *Modern solar facilities - advanced solar science*, 359 (2007).

62. Bazarghan, M., Safari, H., Innes, D. E., Karami, E. & Solanki, S. K. A nanoflare model for active region radiance: application of artificial neural networks. *aap* **492**, L13–L16, DOI: 10.1051/0004-6361:200810911 (2008).

63. Hudson, H. S. Solar flares, microflares, nanoflares, and coronal heating. *solphys* **133**, 357–369, DOI: 10.1007/BF00149894 (1991).

64. Crosby, N. B., Aschwanden, M. J. & Dennis, B. R. Frequency distributions and correlations of solar X-ray flare parameters. *solphys* **143**, 275–299, DOI: 10.1007/BF00646488 (1993).

65. Krucker, S. & Benz, A. O. Energy Distribution of Heating Processes in the Quiet Solar Corona. *apjl* **501**, L213–L216, DOI: 10.1086/311474 (1998).

66. Parnell, C. E. & Jupp, P. E. Statistical Analysis of the Energy Distribution of Nanoflares in the Quiet Sun. *apj* **529**, 554–569, DOI: 10.1086/308271 (2000).

67. Wheatland, M. S. & Litvinenko, Y. E. Energy Balance in the Flaring Solar Corona. *apj* **557**, 332–336, DOI: 10.1086/321655 (2001).

68. Klimchuk, J. A., Reale, F., Testa, P. & Parenti, S. Observations of Nanoflare Produced Hot (10 Mk) Plasma. In *AAS/Solar Physics Division Meeting #40*, vol. 40 of *AAS/Solar Physics Division Meeting*, 12.14 (2009).

69. Fletcher, L. *et al.* An Observational Overview of Solar Flares. *ssr* **159**, 19–106, DOI: 10.1007/s11214-010-9701-8 (2011).

70. Reale, F. Coronal Loops: Observations and Modeling of Confined Plasma. *Living Rev. Sol. Phys.* **11**, 4, DOI: 10.12942/lrsp-2014-4 (2014).

71. Hosseini Rad, S., Alipour, N. & Safari, H. Energetics of Solar Coronal Bright Points. *apj* **906**, 59, DOI: 10.3847/1538-4357/abc8e8 (2021).

72. Sornette, A. & Sornette, D. Self-organized criticality and earthquakes. *EPL (Europhysics Lett.* **9**, 197, DOI: 10.1209/0295-5075/9/3/002 (1989).

73. Biondo, A. E., Pluchino, A. & Rapisarda, A. Modeling financial markets by self-organized criticality. *Phys. Rev. E* **92**, 042814, DOI: 10.1103/PhysRevE.92.042814 (2015).

74. Jr., F. J. M. The kolmogorov-smirnov test for goodness of fit. *J. Am. Stat. Assoc.* **46**, 68–78, DOI: 10.1080/01621459.1951.10500769 (1951).

75. Miller, L. H. Table of percentage points of kolmogorov statistics. *J. Am. Stat. Assoc.* **51**, 111–121, DOI: 10.1080/01621459.1956.10501314 (1956).

76. Marsaglia, G., Tsang, W. W. & Wang, J. Evaluating kolmogorovs distribution. *J. Stat. Softw.* **8**, 14, DOI: 10.18637/jss.v008.i18 (2003).